Periodic Mesoporous Organosilicas with Ethane and Large Isocyanurate Bridging Groups

Rafal M. Grudzien,[†] Bogna E. Grabicka,[†] Stanisław Pikus,[‡] and Mietek Jaroniec*,[†]

Department of Chemistry, Kent State University, Kent, Ohio 44242, and Department of Crystallography, M. Curie-Skłodowska University, 20-031 Lublin, Poland

Received December 8, 2005
Revised Manuscript Received February 5, 2006

Impressive progress has been made in the area of ordered mesoporous materials since the first report on the self-assembly of cationic surfactants and silica species.[1] One of the most exciting achievements in this area was the discovery of periodic mesoporous organosilicas (PMOs).[2] They form a unique class of hybrid materials synthesized by using ionic surfactants,[2] oligomeric surfactants,[3] and nonionic block copolymers[4,5] as structure directing agents, in which organic moieties are integrated into a silica framework. As a result of a great easiness of incorporation of various organic bridging groups into silica framework and their uniform distribution inside walls of ordered mesopores, PMOs[2−5] became very promising materials for the design of highly selective adsorbents, catalysts, and sensing devices as well as for immobilization and encapsulation of biomolecules. So far, research on PMOs was mainly focused on the incorporation of small aliphatic and aromatic bridging groups such as methylene, ethane, ethylene, phenylene, and thiophene into PMOs by using both ionic surfactants and nonionic block copolymers.[2−7] Later, numerous attempts have been made to incorporate larger organic spacers into PMOs such as bipyridine, biphenylene, teraazacyclotetradecane, and the benzene ring linked to three silicon atoms.[8] These attempts stimulated others[9] to synthesize PMOs with large bridging groups such as isocyanurate ring by co-condensation of tri-[3-(trimethoxysilyl)propyl]isocyanurate (ICS) with tetraethyl orthosilicate (TEOS) in the presence of block copolymer under highly acidic conditions. The resulting materials exhibited high surface area, high concentration of incorporated bridging groups, and good structural ordering.[9]

There is a growing interest in the synthesis of PMOs that contain more than one functional group because a proper selection of these groups allows one to design multifunctional nanomaterials for specific catalytic, environmental, and related applications. Bifunctional PMOs with one small bridging group and one surface ligand have been already prepared by either post-synthesis grafting or co-condensation;[10] however, there are only a few reports on the synthesis of bifunctional PMOs with two relatively small bridging groups, for example, ethane and benzene.[11] Recently, a bifunctional PMO with a large isocyanurate bridging group and mercaptopropyl surface group was synthesized by co-condensation of two organosilanes containing those groups and TEOS.[12]

Here we report the synthesis of a new bifunctional PMO, which was synthesized without TEOS and contains two types of bridging groups, ethane and isocyanurate (see Scheme 1). The core of the latter large group is an isocyanurate ring integrated with three silicon atoms through flexible propyl chains. The aforementioned PMO was synthesized by co-condensation of ICS and 1,2-bis(triethoxysilyl)ethane (BTSE) in the presence of a triblock copolymer as the structure directing agent at low acid concentrations.

Bifunctional ethane- and isocyanurate-bridged PMOs were prepared by co-condensation using BTSE (97%, Gelest) and ICS (Aldrich) in the presence of poly(ethylene oxide)−poly-(propylene oxide)−poly(ethylene oxide) triblock copolymer

* To whom the correspondence should be addressed. Phone: 330 672 3790. E-mail: jaroniec@kent.edu.
[†] Kent State University.
[‡] M. Curie-Skłodowska University.

(1) Kresge, C. T.; Leonowicz, M. E.; Roth, W. J.; Vartuli, J. C.; Beck, J. S. *Nature* **1992**, 359, 710.
(2) Inagaki, S.; Guan, S.; Fukushima, Y.; Ohsuna, T.; Teresaki, O. *J. Am. Chem. Soc.* **1999**, *121*, 9611. Melde, B. J.; Holland, B. T.; Blandford, C. F.; Stein, A. *Chem. Mater.* **1999**, *11*, 3302. Asefa, T.; MacLachlan, M. J.; Coombos, N.; Ozin, G. A. *Nature* **1999**, *402*, 867. Yoshina-Ishii, C.; Asefa, T.; Coombos, N.; MacLachlan, M. J.; Ozin, G. *Chem. Commun.* **1999**, 2539.
(3) Lu, Y.; Fan, H.; Doke, N.; Loy, D. A.; Assink, R. A.; LaVan, D. A.; Brinker, C. J. *J. Am. Chem. Soc.* **2000**, *122*, 5258. McInall, M. D.; Scott, J.; Mercier, L.; Kooyman, P. J. *Chem. Commun.* **2001**, 2282. Fan, H.; Reed, S.; Bear, T.; Schunk, R.; Lopez, G. P.; Brinker, C. J. *Microporous Mesoporous Mater.* **2001**, *44*, 625. Dag, O.; Ozin, G. A. *Adv. Mater.* **2001**, *13*, 1182. Dag, O.; Yoshina-Ishii, C.; Asefa, T.; MacLachlan, M. J.; Grondley, H.; Coombos, N.; Ozin, G. A. *Adv. Funct. Mater.* **2001**, *11*, 213.
(4) Matos, J. R.; Kruk, M.; Mercuri, L. P.; Jaroniec, M.; Asefa, T.; Coombos, N.; Ozin, G. A.; Teresaki, O. *Chem. Mater.* **2002**, *14*, 1903.
(5) Bao, X. Y.; Zhao, X. S.; Li, X.; Chia, P. A.; Li, J. *J. Phys. Chem. B* **2004**, *108*, 4684. Bao, X. Y.; Zhao, X. S. *J. Phys. Chem. B* **2005**, *109*, 10727.
(6) Zhu, H.; Jones, D. J.; Zajac, J.; Dutartre, R. *Chem. Commun.* **2001**, 2568. Sayari, A.; Hamoudi, S.; Yang, Y.; Moudarovski, I. L.; Ripmeester, J. R. *Chem. Mater.* **2000**, *12*, 3857. Muth, O.; Schellbach, C.; Froeba, M. *Chem. Commun.* **2001**, 2032. Inagaki, S.; Guan, S.; Ohsuna, T.; Teresaki, O. *Nature* **2002**, *416*, 204. Li, Y.; Yang, L.; Liu, J.; Li, C. *J. Phys. Chem. B* **2004**, *108*, 7034.
(7) Asefa, T.; Yoshina-Ishii, C.; MacLaclan, M.; Ozin, G. A. *J. Mater. Chem.* **2000**, *10*, 1751. Sayari, A.; Hamoudi, S. *Chem. Mater.* **2001**, *13*, 3151. Kickkelbick, G. *Angew. Chem., Int. Ed.* **2004**, *43*, 3102. Hatton, B.; Landskron, K.; Whitnall, W.; Perovic, D.; Ozin, G. A. *Acc. Chem. Res.* **2005**, *38*, 305. Vinu, A.; Hossain, K. Z.; Ariga, K. *J. Nanosci. Nanotechnol.* **2005**, *5*, 347. Ford, D. M.; Simanek, E. E.; Shantz, D. F. *Nanotechnology* **2005**, *16*, 458.
(8) Kapoor, M. P.; Yang, Q.; Inagaki, S. *J. Am. Chem. Soc.* **2002**, *124*, 15176. Corriu, R. J. P.; Mehedi, A.; Reye, C.; Thieuleux, C. *Chem. Commun.* **2002**, 1382. Kuroki, M.; Asefa, T.; Whitnal, W.; Kruk, M.; Yoshina-Ishii, C.; Jaroniec, M.; Ozin, G. A. *J. Am. Chem. Soc.* **2002**, *124*, 13886. Llandskrn, K.; Hhatton, B. D.; Pervic, D. D.; Ozin, G. A. *Science* **2003**, *302*, 266.
(9) Olkhovyk, O.; Jaroniec, M. *J. Am. Chem. Soc.* **2005**, *127*, 60.
(10) Burleigh, M. C.; Sheng, D.; Hagaman, E. W.; Lin, J. S. *Chem. Mater.* **2001**, *13*, 2537. Asefa, T.; Kruk, M.; MacLachlan, M. J.; Coombos, N.; Grondey, H.; Jaroniec, M.; Ozin, G. A. *J. Am. Chem. Soc.* **2001**, *123*, 8520. Burleigh, M. C.; Markowitz, M. A.; Spector, M. S.; Gaber, B. P. *Chem. Mater.* **2001**, *13*, 4760. Burleigh, M. C.; Markowitz, M. S.; Spector, M. S.; Gaber, B. P. *Langmuir* **2001**, *17*, 7923. Burleigh, M. C.; Markowitz, M. S.; Spector, M. S.; Gaber, B. P. *J. Phys. Chem. B* **2001**, *105*, 9935. Yang, Q. H.; Liu, L.; Yang, J. *J. Catal.* **2004**, *228*, 265. Tshavhungwe, A. M.; Layh, M.; Coville, N. J. *J. Sol.-Gel Sci. Technol.* **2004**, *29*, 167. Wahab, A.; Kim, II.; Ha, C.-S. *Microporous Mesoporous Mater.* **2004**, *69*, 19.
(11) Burleigh, M. C.; Jayaundera, S.; Spector, M. S.; Thomas, C. W.; Markowitz, M. A.; Gaber, B. P. *Chem. Mater.* **2004**, *16*, 3. Jayaundera, S.; Burleigh, M. C.; Zeinali, M.; Spector, M. S.; Miller, J. B.; Yan, W.; Dai, S.; Markowitz, M. A. *J. Phys. Chem. B* **2005**, *109*, 9198.
(12) Olkhovyk, O.; Pikus, S.; Jaroniec, M. *J. Mater. Chem.* **2005**, *15*, 1517.

10.1021/cm052717x CCC: $33.50
Published on Web 03/03/2006

Scheme 1. Schematic Illustration of Bifunctional PMO with Ethane and Isocyanurate Bridging Groups[a]

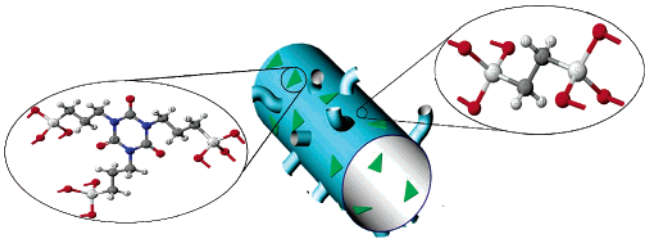

[a] The triangles illustrate isocyanurate bridging groups incorporated into the ethane−silica framework, whereas curved pipes represent microporous interconnections between ordered mesopores.

Table 1. Synthesis Gel Compositions, Elemental Analysis Data, and TG Weight Loss Data for the PMOs Studied[a]

			elemental analysis		
sample	*x* ICS	n_t (mmol)	%C	%N	TG wt loss (%)
EI-0	0	5.16	19.12	0	17.42
EI-1	0.07	4.99	22.28	2.42	26.85
EI-2	0.14	4.82	23.94	2.74	28.22
EI-3	0.22	4.65	26.73	4.37	34.96

[a] Notation: *x*, mole fraction of ICS in the synthesis gel; n_t, total number of mmoles of BTSE and ICS in the synthesis gel; TG, weight loss recorded in flowing air in the range from 100 to 950 °C.

(Pluronic P123, $EO_{20}PO_{70}EO_{20}$, BASF) at low acid concentrations. In a typical synthesis, analogous to that by Bao et al.,[5] 7 mL of deionized water (DW) was combined with 0.5 g of triblock copolymer P123 and stirred at 40 °C to form a clear solution. A specified amount of BTSE (see Table 1) was added to a solution containing 1.8 mL of DW and 0.6 mL of 2 M HCl at 40 °C. The P123−DW solution was then slowly added to the BTSE−DW−HCl mixture under vigorous stirring, and then after 15 min, ICS was added dropwise to achieve the desired molar composition of both silanes. After further stirring for 24 h at 40 °C, the resulting white precipitate was transferred into a polypropylene bottle and subsequently heated at 100 °C for 48 h. The product was filtered, washed with DW, and dried in the oven at 80 °C. The molar composition of the BTSE and ICS in the synthesis gel was $(1 - x)$ BTSE:*x* ICS, where *x* denotes the mole fraction of ICS. The amount of the BTSE used was adjusted to maintain the Si/polymer ratio at the same level for the samples studied. The as-synthesized nanocomposites were extracted twice with 2 mL of HCl and 100 mL of 95% EtOH at 70 °C to remove the polymeric template from the mesopores. The extracted PMOs are denoted as EI-*z*, where E and I denote ethane and isocyanurate bridging groups, respectively, and *z* denotes the sample number. PMO with $z = 0$ refers to the pure ethane−silica. For the samples with growing *z* the ICS mole fraction increases as shown in Table 1.

The structure of the extracted bifunctional PMOs was studied by small-angle X-ray scattering (SAXS). The SAXS profiles are shown in Figure 1. As can be seen from Figure 1 the SAXS pattern for the pure ethane-bridged PMO depicted as EI-0 shows three sharp reflections indexed as (100), (110), and (200) that are typical for two-dimensional hexagonal structure (*P*6*mm* symmetry group). For the sample with a small concentration of ICS (EI-1) the SAXS pattern

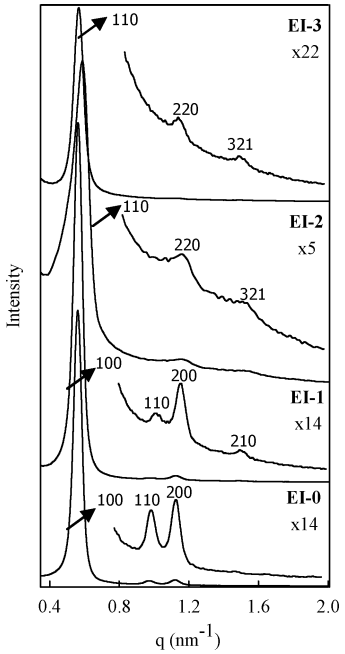

Figure 1. Comparison of SAXS patterns for a series of the extracted PMOs studied.

is still characteristic for the *P*6*mm* symmetry group although the intensity of the (110) peak decreased (see Supporting Information, Table 1S). However, for PMOs with a higher amount of ICS (samples EI-2 and EI-3) the SAXS patterns are different. In this case a complete lack of the (110) peak characteristic for the *P*6*mm* symmetry group, important for its identification, is observed. In addition, a new reflection at the scattering vector $q = 1.5$ is visible on the SAXS patterns for the EI-2 and EI-3 samples, which is not present on the pattern for EI-0, despite a general deterioration of the quality of these patterns. Thus, the SAXS data suggest a structural change in the symmetry group with increasing concentration of ICS in PMO. Analogous structural changes were observed for other PMOs.[12] Because only three reflections are present on the SAXS patterns for the EI-2 and EI-3 PMOs, a precise determination of the symmetry group cannot be made. On the other hand, the lack of a (110) reflection characteristic for *P*6*mm* and the appearance of a new reflection for these PMOs permits the existing reflections to be assigned as (110), (220), and (321) according to the $I4_132$ cubic symmetry group (see structural parameters in Supporting Information, Table 2S).

A comparison of nitrogen adsorption isotherms measured at −196 °C for the bifunctional PMOs studied is shown in Figure 2A. These isotherms are type IV with steep capillary condensation/evaporation steps and H1 hysteresis loops. They were used to evaluate the BET specific surface area, volume of fine pores (i.e., pores below 4 nm), volume of primary mesopores, and mesopore diameter, which are in Table 2. The corresponding pore size distributions (PSDs; Figure 2B), evaluated by the KJS (Kruk, Jaroniec, and Sayari) method,[13] are narrow, indicating high uniformity of ordered mesopores. As can be seen from Figure 2 and Supporting Information, Figure 1SA, the isotherm curves and the corresponding PSDs

(13) Kruk, M.; Jaroniec, M.; Sayari, A. *Langmuir* **1997**, *13*, 6267.

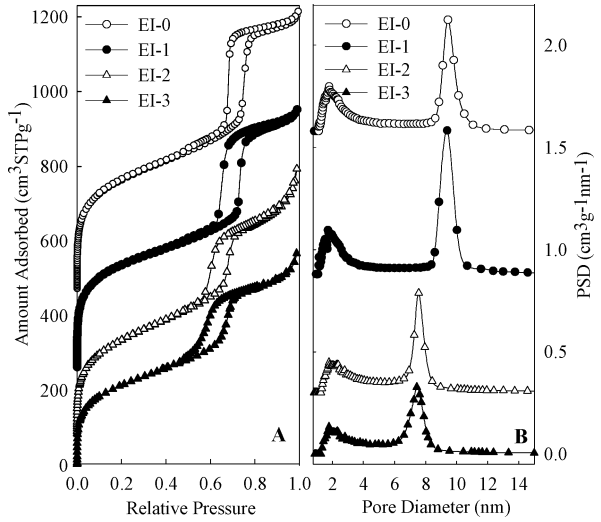

Figure 2. (A) Comparison of nitrogen adsorption−desorption isotherms at −196 °C for a series of the extracted PMOs. The isotherms for EI-2, EI-1, and EI-0 were offset vertically by 86, 263, and 437 cm^3 STP g^{-1}, respectively. (B) The corresponding PSDs calculated according to the KJS method; PSDs for EI-2, EI-1, and EI-0 were shifted by 0.3, 0.88, and 1.58 cm^3 g^{-1} nm^{-1}, respectively.

Table 2. Adsorption Properties of PMOs Determined from Nitrogen Adsorption Data[a]

sample	S_{BET} (m^2 g^{-1})	V_m (cm^3 g^{-1})	V_p (cm^3 g^{-1})	V_t (cm^3 g^{-1})	w_{KJS} (nm)
EI-0	1068	0.33	0.75	1.14	9.43
EI-1	997	0.30	0.69	1.05	8.86
EI-2	933	0.27	0.61	1.05	7.56
EI-3	773	0.21	0.51	0.85	7.44

[a] S_{BET}, BET specific surface area; V_m, volume of pores below 4 nm; V_p, volume of primary pores calculated between 4 and 12 nm; V_t, single-point pore volume; w_{KJS}, mesopore diameter.

change gradually for the PMOs studied from EI-0 to EI-3. For this series of PMOs the BET surface area, pore volume, and pore size decrease with increasing concentration of the ICS bridging groups. In addition, the condensation/evaporation steps become less sharp with increasing concentration of ICS, which suggests a gradual deterioration of the mesoporous structure. This is expected because of the geometrical constrictions to accommodate a large number of bulky ICS bridging groups in the mesopore walls. Moreover, adsorption isotherms (see Figure 2A and Supporting Information, Figure 1S) do not level off at relative pressures above 0.8 but rise, and this rising intensifies with increasing concentration of ICS, which reflects a gradual development of textural porosity, that is, secondary disordered mesopores. Note that PSDs (see Figure 2B and Supporting Information, Figure 2S) contain also a distinct peak in the pore range below 4 nm indicating the presence of micropores and small mesopores that are formed because of penetration of some polyethylene (EO) blocks into the silica wall.[14] As a result of the large size of ICS, at its higher concentration the ICS groups occupy more space of the mesopore walls of ethane−silica, which results in the reduction of space available for the aforementioned EO penetration[14] that is equivalent to the reduction of micropore volume (see Table 2).

(14) Ryoo, R.; Ko, C. H.; Kruk, M.; Antochshuk, V.; Jaroniec, M. *J. Phys. Chem. B* **2000**, *104*, 11465.

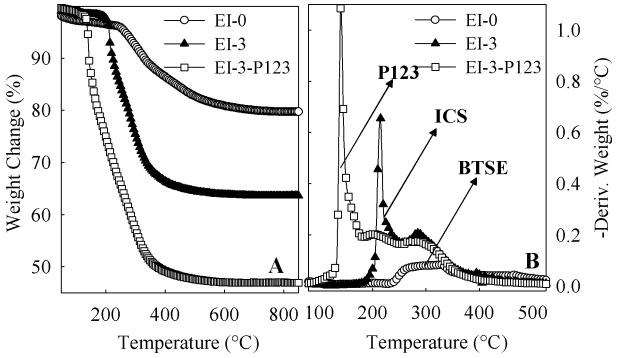

Figure 3. (A) Comparison of the TG weight change curves measured in flowing air for as-synthesized (EI-3-P123) and extracted (EI-0 and EI-3) PMOs and (B) the corresponding DTG curves.

While a gradual change in the adsorption properties was observed for a series of PMOs from EI-0 to EI-1, this was not the case for two PMOs synthesized using the ICS concentration lower than that for EI-1. As can be seen from Supporting Information, Figures 1SB and 2S, the isotherm and PSD curves for those samples do not lie between that for EI-0 and that for EI-1. The pore volume and pore size for the EI-a and EI-b PMOs are smaller than the corresponding values for EI-1 (see Supporting Information, Table 3S). Also, there was a tendency to create higher textural (secondary) mesoporosity at low concentrations of ICS. Because analogous irregularity (unpublished data) was observed for other PMOs with large bridging groups, we hypothesize that a threshold concentration of these groups is required to achieve their uniform distribution in the entire sample. To achieve a relatively good uniformity of PMOs at low concentrations of large bridging groups their mesopore walls should be thicker and the volume of primary mesopores should be smaller. Although these features are observed for the EI-a and EI-b samples, further studies are required to verify the aforementioned hypothesis.

The incorporation of large heterocyclic groups to the ethane−silica was monitored by high resolution thermogravimetry (TG) for the EI-0, EI-3, and EI-3-P123 samples; the latter contains polymer template. The TG profiles and the corresponding differential TG (DTG) curves recorded in flowing air are shown in Figure 3. The TG weight loss data for the extracted bifunctional PMOs are given in Table 1. The DTG curves for the extracted bifunctional PMOs (see curve for EI-3 in Figure 3B) exhibit two decomposition peaks appearing in the temperature ranges of 180−250 °C and 250−400 °C, which can be attributed to the thermal degradation of cross-linked heterocyclic rings and ethane bridging groups, respectively. A successful removal of P123 triblock copolymer by extraction is confirmed by the disappearance of the characteristic decomposition peak at about 160 °C (see the DTG curve for the EI-3-P123 sample in Figure 3B).

To determine the effect of thermal degradation of isocyanurate and ethane bridging groups on the mesostructure, the extracted sample (EI-2) calcined in flowing air at 550 °C was investigated by nitrogen adsorption and powder X-ray diffraction (see Supporting Information, Figures 3S, 4S, and 5S). As can be seen from these figures the thermal removal of bridging groups did not lead to the collapse of mesoporous

structure and even retained its ordered nature; however, a substantial reduction in the pore volume, pore width, and surface area was observed, which is not surprising as a result of the structure shrinkage and a complete elimination of bulky isocyanurate bridging groups as well as ethane groups from the PMO framework caused by calcination of the sample in flowing air (see Supporting Information, Table 4S).

The concentration of incorporated isocyanurate rings in the mesopore walls of ethane−silica was estimated by elemental analysis (see %N and %C values in Table 1). Nitrogen and carbon percentages obtained from elemental analysis, for example, for EI-3 (%N = 4.37 and %C = 26.73), are very close to the values estimated on the basis of the synthesis gel composition (%N = 4.83 and %C = 26.21), which confirms a good incorporation of a large bridging ICS group to the ethane−silica framework.

In summary, this work shows that bifunctional PMOs can be synthesized by incorporation of large bridging groups such as isocyanurate rings into ethane−silica. The high quality PMOs with relatively large concentration of bulky bridging groups were obtained in terms of the framework periodicity, high pore volume, and high surface area.

Acknowledgment. The authors acknowledge support by NSF Grant CHE-0093707.

Supporting Information Available: SAXS and adsorption parameters, nitrogen adsorption−desorption isotherms, PSDs, and X-ray diffraction patterns (PDF). This material is available free of charge via the Internet at http://pubs.acs.org.

CM052717X